Available online at www.sciencedirect.com
SCIENCE DIRECT®
Journal of Sound and Vibration 286 (2005) 97–122
JOURNAL OF SOUND AND VIBRATION
www.elsevier.com/locate/jsvi

Efficiency and tuning of viscous dampers on discrete systems

Joseph A. Main, Steen Krenk*

Department of Mechanical Engineering, Technical University of Denmark, Building 403, DK-2800 Kgs. Lyngby, Denmark

Received 14 April 2004; received in revised form 23 September 2004; accepted 29 September 2004
Available online 24 December 2004

Abstract

An approximate solution is developed to the complex eigenproblem associated with free vibrations of a discrete system with several viscous dampers, in order to facilitate optimal placement and sizing of added dampers in structures. The approximate solution is obtained as an interpolation between the solutions of the two limiting eigenproblems: the undamped eigenproblem and the constrained eigenproblem in which each damper is replaced with a rigid link. An explicit form of the approximate solution is developed for cases in which the difference between these limiting eigensolutions is sufficiently small, and an iterative solution scheme is presented for cases in which the difference is larger. These results allow the efficiency and tuning of viscous dampers to be investigated by solving only the two limiting real-valued eigenproblems. The application of the approximate formulation is illustrated for a 10-story building model with added dampers.

1. Introduction

The response of a structure to dynamic loading depends strongly on the capacity of the structure to dissipate energy. Because the inherent damping in many structures is quite low, significant advantage can be gained by providing additional dissipation, and in recent decades, supplemental energy dissipation devices have emerged as an economical alternative to structural stiffening for improving the performance of engineered structures [1]. Examples of passive energy dissipation devices include friction dampers, viscoelastic dampers, and viscous fluid dampers [2].

*Corresponding author. Tel.: +45 4525 1964; fax: +45 4588 4325.
E-mail addresses: jmain@jhu.edu (J.A. Main), sk@mek.dtu.dk (S. Krenk).

0022-460X/$ - see front matter © 2004 Elsevier Ltd. All rights reserved.
doi:10.1016/j.jsv.2004.09.022

Supplemental dampers have been employed in a variety of contexts, including seismic protection of buildings [3], suppression of stay-cable vibrations in bridges [4], and mitigation of traffic-induced vibrations in a pedestrian bridge [5]. While the focus of the present study is on passive dampers, active damping devices have also found increasing application in structures (see e.g. Ref. [6]).

Effective tuning of supplemental dampers to optimize their efficiency requires an accurate representation of the influence of the dampers on the dynamics of the structure. In the present paper, this influence is investigated by considering the dynamic characteristics of a general discrete system with several linear viscous dampers. Although supplemental damping devices commonly exhibit nonlinear and nonviscous characteristics, linear viscous damping is the simplest form of damping to represent analytically, and the effect of nonlinearity can often be represented with fair accuracy by equivalent linearization based on equivalent energy dissipation at a representative frequency and amplitude level.

While the assumption of classical damping (also called *proportional damping*) is commonly employed in the dynamic analysis of structures, this assumption is generally not justified for structures with supplemental dampers. In classically damped systems, the mode shapes are unaffected by the damping forces, allowing the equations of motion to be transformed into a set of independent modal equations using the real-valued mode shapes of the undamped system. For such decoupling to occur, the distribution of damping in the structure must match the distribution of mass and stiffness through the condition established by Caughey and O'Kelly [7]. Supplemental dampers are commonly attached at a few distinct locations within the structure, so that the damping forces do not match the mass or stiffness distribution. Consequently, the undamped mode shapes generally do not uncouple the equations of motion for structures with added dampers.

Another common assumption in representing damping, which does not restrict the distribution of damping forces, is that the structure is lightly damped (see e.g. Refs. [8,9]). In this approach, which dates back to Rayleigh [10], the damping forces are assumed to be an order of magnitude smaller than the inertial and stiffness forces, and the damping-induced perturbations of the eigenfrequencies and mode shapes and are also assumed small. Under these assumptions, each eigenfrequency is modified by an imaginary part that reflects the dissipation in the undamped mode shape, and each mode shape is modified by an imaginary part that is orthogonal to the undamped mode shape. While these assumptions of light damping are usually justified for inherent damping forces in structures, supplemental damping devices are capable of producing large forces that can be of comparable magnitude to the inertial and stiffness forces. The large, localized forces produced by supplemental dampers thus have the potential to perturb the mode shapes and eigenfrequencies in ways that cannot be represented through the assumptions of classical damping or of light damping.

In the general case of viscous damping with unrestricted magnitude and distribution, a method of dynamic analysis using complex modes is well established, having been developed for discrete systems by Foss [11]. More recently Krenk [12] developed a corresponding formulation for the damped vibrations of continuous systems. In these methods, the complex eigenvalues and mode shapes are first evaluated from the homogeneous problem corresponding to free vibrations. Orthogonality properties of the complex mode shapes then enable a transformation of the equations of motion to a set of uncoupled modal equations, and the forced response of the system

can be expressed as a superposition of the modal responses, in a fairly straightforward extension of classical modal analysis.

In the design of supplemental dampers for structures, it is often desirable to optimize the placement and sizing of the dampers to minimize response quantities such as displacements, accelerations, and internal forces. In some cases, the responses in a few specific modes of vibration are known to be of greatest concern, and rather than optimizing the dampers for a specific loading function, the dampers can be designed to provide specified levels of damping in these problematic modes, or perhaps to provide the maximum possible damping in a particular mode. Because values of modal damping are determined directly from the complex eigenvalue problem corresponding to free vibrations, this approach considerably simplifies the design optimization problem, eliminating the need to evaluate forced responses at each step in the optimization. However, even this simpler approach can be time-consuming for large structures, requiring repeated solving of a complex eigenvalue problem of large dimension in order to determine the optimal location and sizing of the added dampers.

In this paper, an approximate solution is developed to the complex eigenproblem associated with free vibrations of a discrete system with several viscous dampers, in order to facilitate optimal placement and sizing of added dampers in structures. The approximate solution is obtained as an interpolation between the solutions of two limiting eigenproblems: the undamped eigenproblem and the constrained eigenproblem in which each damper is replaced with a rigid link. Preumont [6] previously used these limiting cases of free and fully locked vibrations to develop approximate solutions for structures with active damping. An explicit expression in the form of a rational function is obtained for cases in which the difference between these limiting eigensolutions is sufficiently small, and an iterative solution scheme is presented for cases in which the difference is larger. The explicit approximation has the same form as the asymptotic approximation originally obtained by Krenk [13] for a taut cable with a viscous damper attached near one end, which was subsequently extended to a sagging cable [14], to rotational dampers at the ends of a beam [12], and to a tensioned beam with a damper near one end [15]. These results allow the efficiency and tuning of viscous dampers to be investigated by solving only the two limiting real-valued eigenproblems, rather than repeatedly solving the complex-valued eigenproblem of the damped system with varying location and sizing of the added dampers. The application of the approximate formulation is illustrated for a 10-story building model with added dampers.

2. Eigenvalue problem and limiting solutions

The equations of motion for free vibrations of an n-degree-of-freedom linear system with viscous damping can be written in the following general form:

$$\mathbf{M}\ddot{\mathbf{q}} + \mathbf{C}\dot{\mathbf{q}} + \mathbf{K}\mathbf{q} = \mathbf{0} \tag{1}$$

where $\mathbf{M}$, $\mathbf{C}$, and $\mathbf{K}$ are the $n \times n$ mass, damping, and stiffness matrices, $\mathbf{q}$ is an $n \times 1$ vector of generalized displacements, and the dot represents differentiation with respect to time t. Expressing solutions to Eq. (1) as

$$\mathbf{q} = \mathrm{Re}[\mathbf{u}\exp(\mathrm{i}\omega t)] \tag{2}$$

yields the quadratic eigenvalue problem

$$(\mathbf{K} + \mathrm{i}\omega\mathbf{C} - \omega^2\mathbf{M})\mathbf{u} = \mathbf{0} \tag{3}$$

Nontrivial solutions require that $\det(\mathbf{K} + \mathrm{i}\omega\mathbf{C} - \omega^2\mathbf{M}) = \mathbf{0}$, and the roots of this characteristic equation are the eigenfrequencies of the system ω_k. The corresponding eigenvectors $\mathbf{u}_k$ are the vibration mode shapes of the system, and both ω_k and $\mathbf{u}_k$ are complex-valued in general. The real part of ω_k gives the frequency of damped oscillation, and the imaginary part gives the rate of decay. Modal damping ratios can be defined as follows, in analogy with the case of classical damping:

$$\zeta_k = \mathrm{Im}[\omega_k]/|\omega_k| \tag{4}$$

Of interest in the present study are damping forces produced by one or more viscous dampers added to the system, and such forces can be represented by a damping matrix $\mathbf{C}$ with the following form (see e.g. Ref. [16]):

$$\mathbf{C} = \sum_{j=1}^{r} c_j \mathbf{w}_j \mathbf{w}_j^{\mathrm{T}} \tag{5}$$

where r is the total number of added dampers, c_j is the viscous coefficient of the jth damper, and the $n \times 1$ vector $\mathbf{w}_j$ represents the attachment position and orientation of the jth damper. Preumont [6] has used a similar format to represent the forces in active structural members.

For the five-story shear building model in Fig. 1, for example, the vector $\mathbf{w}_1$ associated with the damper attached between the first floor and the fixed ground is given by

$$\mathbf{w}_1 = [1 \quad 0 \quad 0 \quad 0 \quad 0]^{\mathrm{T}} \tag{6}$$

while the vector $\mathbf{w}_2$ associated with the damper attached between the third and fourth floors is given by

$$\mathbf{w}_2 = [0 \quad 0 \quad -1 \quad 1 \quad 0]^{\mathrm{T}} \tag{7}$$

The form of Eq. (5) can thus accommodate dampers attached between two degrees of freedom within the system, which produce forces due to relative motion, as well as dampers attached

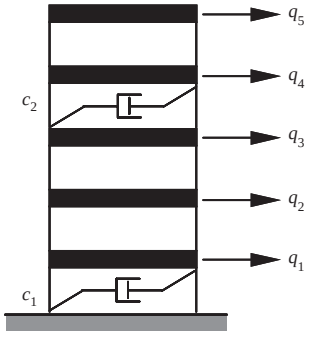

Fig. 1. Five-story shear building with two viscous dampers.

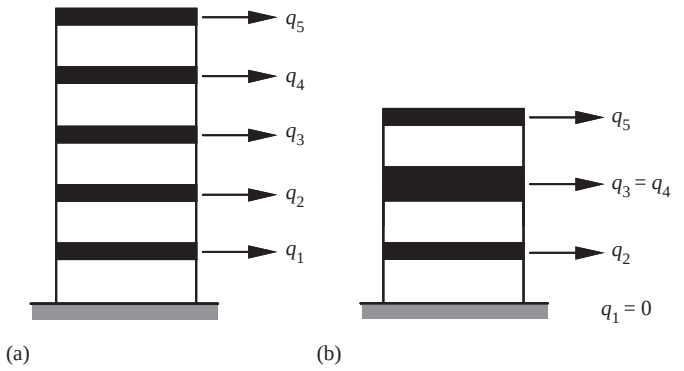

Fig. 2. Limiting cases for the system of Fig. 1: (a) undamped system ($c_1 = c_2 = 0$); (b) constrained system ($c_1, c_2 \to \infty$).

between a degree of freedom and a fixed external reference, which produce forces due to absolute motion.

In investigating the nature of the complex eigenfrequencies and eigenvectors resulting from Eq. (3) with the special form of damping in Eq. (5), it is helpful to first consider the solutions in the limiting cases corresponding to those depicted Fig. 2 for the damped shear building model of Fig. 1. The first limiting case corresponds to setting all the damper coefficients c_j to zero, for which the system simply reduces to the undamped case, as depicted in Fig. 2(a). The second limiting case corresponds to letting $c_j \to \infty$ for all dampers, which results in a constrained system, as depicted in Fig. 2(b). The characteristics of these limiting systems and their eigensolutions are discussed in the following sections.

2.1. Undamped system

In the first limiting case, when $c_j = 0$ for each damper in the system, Eq. (3) reduces to the following familiar undamped eigenvalue problem:

$$(\mathbf{K} - \omega_0^2 \mathbf{M})\mathbf{u}_0 = \mathbf{0} \tag{8}$$

where the subscript 0 denotes the undamped system. For nontrivial solutions $\det(\mathbf{K} - \omega_0^2 \mathbf{M}) = \mathbf{0}$, and the roots of this characteristic equation are the real-valued undamped eigenfrequencies ω_{0k}, with corresponding real-valued eigenvectors $\mathbf{u}_{0k}$, where the index k denotes the mode number, $k = 1, 2, \ldots, n$. For convenience, each undamped eigenvector $\mathbf{u}_{0k}$ can be normalized such that

$$\mathbf{u}_{0k}^{\mathrm{T}} \mathbf{M} \mathbf{u}_{0k} = 1, \quad \mathbf{u}_{0k}^{\mathrm{T}} \mathbf{K} \mathbf{u}_{0k} = \omega_{0k}^2 \tag{9}$$

It follows from Eq. (8) that the undamped mode shapes also satisfy the well-known orthogonality conditions: $\mathbf{u}_{0l}^{\mathrm{T}} \mathbf{M} \mathbf{u}_{0k} = 0$ and $\mathbf{u}_{0l}^{\mathrm{T}} \mathbf{K} \mathbf{u}_{0k} = 0$ for $\omega_{0l}^2 \neq \omega_{0k}^2$.

2.2. Constrained system

In the second limiting case, as $c_j \to \infty$ for each damper in the system, the dampers act as rigid links, introducing constraints on the motion of the system but providing no dissipation. One

constraint equation is introduced for each rigid link in the system, and because the attachment position of the jth link is represented by the vector $\mathbf{w}_j$, these constraint equations can be written in the following form:

$$\mathbf{u}_\infty^{\mathrm{T}}\mathbf{w}_j = 0, \quad j = 1, \ldots, r \tag{10}$$

where the subscript ∞ denotes the constrained system with locked dampers, and the mode number for the eigenvector $\mathbf{u}_\infty$ is not indicated explicitly because any eigenvector of the constrained system must satisfy these equations. These r linear constraint equations reduce the number of degrees of freedom and thus the number of eigensolutions to $(n-r)$. Because the equations of motion (1) have been formulated in terms of n generalized coordinates, the constraint forces in the rigid links appear in the eigenvalue problem for the constrained system as follows:

$$(\mathbf{K} - \omega_\infty^2\mathbf{M})\mathbf{u}_\infty + \mathbf{R} = 0 \tag{11}$$

where $\mathbf{R}$ is a vector of reaction forces produced by the rigid links. This constrained eigenvalue problem yields real-valued eigenfrequencies $\omega_{\infty k}$ and corresponding real-valued eigenvectors $\mathbf{u}_{\infty k}$, where the index k denotes the mode number, $k = 1, 2, \ldots, (n-r)$. In solving the eigenvalue problem (11), the r constraint equations (10) can be used to reduce the number of generalized coordinates to $(n-r)$, thus eliminating the reaction forces and yielding an eigenvalue problem of reduced size with the same form as the undamped eigenvalue problem (8).

In the system of Fig. 1, for example, locking of the dampers introduces two constraints, which can be expressed as $q_1 = 0$ and $q_3 = q_4$. As depicted in Fig. 2(b), these constraints reduce the number of degrees of freedom from five to three. Selecting the three generalized coordinates q_2, q_3, and q_5 then eliminates the necessity of including constraint forces in the equations of motion. Using these coordinates leads to an eigenvalue problem in the form of Eq. (8) with dimension three, where the mass associated with q_3 is the sum of the masses associated with q_3 and q_4 in the original system. The eigenvectors computed from this reduced-dimension problem can then be expanded to the full dimension of the original problem by simply setting $q_1 = 0$ and $q_3 = q_4$ in the (5×1) vectors $\mathbf{u}_{\infty k}$.

Once $\omega_{\infty k}$ and $\mathbf{u}_{\infty k}$ have been determined in a given mode k, the reaction forces associated with that mode, which will prove useful subsequently, can be determined from Eq. (11) as follows:

$$\mathbf{R}_k = (\omega_{\infty k}^2\mathbf{M} - \mathbf{K})\mathbf{u}_{\infty k} \tag{12}$$

This vector of reaction forces can be expanded in terms of the r independent constraint forces in the rigid links as follows:

$$\mathbf{R}_k = \sum_{j=1}^{r} \rho_{kj}\mathbf{w}_j \tag{13}$$

where ρ_{kj} is the constraint force in the jth rigid link for vibrations in mode k. Provided that the dampers are not placed in a redundant manner, the r vectors $\mathbf{w}_j$ are linearly independent, allowing the r constraint forces ρ_{kj} associated with mode k to be uniquely determined from the following equation, obtained by combining Eqs. (12) and (13), and expressing the summation in Eq. (13) as a matrix product:

$$[\,\mathbf{w}_1 \quad \cdots \quad \mathbf{w}_r\,][\,\rho_{k1} \quad \cdots \quad \rho_{kr}\,]^{\mathrm{T}} = (\omega_{\infty k}^2\mathbf{M} - \mathbf{K})\mathbf{u}_{\infty k} \tag{14}$$

Because constraint forces do no work through displacements consistent with the constraints, the product $\mathbf{u}_{\infty l}^{\mathrm{T}}\mathbf{R}_k$ must be zero for any indices k and l, as is readily shown from Eqs. (10) and (13). Premultiplication of Eq. (12) by $\mathbf{u}_{\infty k}^{\mathrm{T}}$ then eliminates the reaction forces, yielding the following equation:

$$\mathbf{u}_{\infty k}^{\mathrm{T}}\mathbf{K}\mathbf{u}_{\infty k} = \omega_{\infty k}^2\mathbf{u}_{\infty k}^{\mathrm{T}}\mathbf{M}\mathbf{u}_{\infty k} \tag{15}$$

As in Eq. (9), each eigenvector $\mathbf{u}_{\infty k}$ can then be normalized such that

$$\mathbf{u}_{\infty k}^{\mathrm{T}}\mathbf{M}\mathbf{u}_{\infty k} = 1, \qquad \mathbf{u}_{\infty k}^{\mathrm{T}}\mathbf{K}\mathbf{u}_{\infty k} = \omega_{\infty k}^2 \tag{16}$$

Premultiplication of Eq. (11) by $\mathbf{u}_{\infty l}^{\mathrm{T}}$ where $k \neq l$ also eliminates the reaction forces, and the same procedure as in the undamped case can then be used to show that the eigenvectors of the constrained system satisfy orthogonality conditions analogous to those in the undamped case: $\mathbf{u}_{\infty l}^{\mathrm{T}}\mathbf{M}\mathbf{u}_{\infty k} = 0$ and $\mathbf{u}_{\infty l}^{\mathrm{T}}\mathbf{K}\mathbf{u}_{\infty k} = 0$ for $\omega_{\infty l}^2 \neq \omega_{\infty k}^2$.

The following property, which will prove useful subsequently, follows from the form of the damping matrix (5) and the fact that the eigenvectors $\mathbf{u}_\infty$ satisfy the constraint equations (10):

$$\mathbf{C}\mathbf{u}_\infty = \mathbf{0} \tag{17}$$

As in Eq. (10) the mode number is not explicitly indicated in Eq. (17) because this property holds for any eigenvector of the constrained system. It also follows from the symmetry of $\mathbf{C}$ that $\mathbf{u}_\infty^{\mathrm{T}}\mathbf{C} = \mathbf{0}$.

3. Approximate solution by interpolation

In developing an approximate solution to the quadratic eigenvalue problem (3) for the damped system, the following approximate representation is assumed for the kth eigenvector, $\tilde{\mathbf{u}}_k \simeq \mathbf{u}_k$:

$$\tilde{\mathbf{u}}_k = \mathbf{u}_{0k} + \alpha_k\mathbf{u}_{\infty k} \tag{18}$$

This linear combination permits exact representation of the limiting eigenvectors, $\mathbf{u}_{0k}$ and $\mathbf{u}_{\infty k}$, by letting $\alpha_k = 0$ and $|\alpha_k| \to \infty$, respectively. For finite damping, Eq. (18) is an approximation, representing an interpolation between these limiting solutions. The accuracy of this interpolative approximation depends on the closeness of the limiting solutions.

In the case of multiple dampers ($r > 1$), the representation (18) implies certain assumptions on the relative sizing of the dampers. While a system with r viscous dampers is being considered, the influence of these dampers on the kth eigenmode is represented in Eq. (18) through a single coefficient, α_k. It is also noted that the limiting eigenvector $\mathbf{u}_{\infty k}$ corresponds to locking of all of the r dampers, as discussed in the previous section. Consequently, the assumed form (18) is unable to represent independent locking of specific dampers; rather, implicit in the form of Eq. (18) is an assumption that all of the dampers lock uniformly as their strength is increased. Also implicit in the form of Eq. (18) is an assumption that all damping forces in a given mode have the same phasing. This uniformity in phasing follows from the fact that $\mathbf{C}\mathbf{u}_{\infty k} = 0$, according to Eq. (17), so that the damping forces $\mathbf{C}\dot{\mathbf{q}}$ resulting from Eq. (18) are proportional to $\mathbf{C}\mathbf{u}_{0k}$, where $\mathbf{u}_{0k}$ is real-valued. It is demonstrated subsequently that these implicit assumptions correspond to a certain condition of proportionality among the r damper coefficients, and approximate conditions are

obtained on the relative sizing implicitly assumed for the dampers. While this assumed proportionality is restrictive, approximation (18) is still quite broadly applicable, because such proportional sizing is often desirable to achieve efficiency, as is observed subsequently in an example.

Because Eq. (18) is an approximation, substitution into Eq. (3) yields an error in the force balance, given by

$$\boldsymbol{\varepsilon}_k = (\mathbf{K} + \mathrm{i}\omega_k \mathbf{C} - \omega_k^2 \mathbf{M})\mathbf{u}_{0k} + \alpha_k(\mathbf{K} - \omega_k^2 \mathbf{M})\mathbf{u}_{\infty k} \tag{19}$$

where the damping matrix $\mathbf{C}$ appears only in the first term of Eq. (19) because of the property in Eq. (17). In formulating the "best" approximation to the kth eigenmode, it is necessary to determine the values of the mode shape coefficient α_k and the eigenfrequency ω_k that minimize this error in some sense. A measure of the energy associated with this error can be obtained by forming the product $\tilde{\mathbf{u}}_k^{\mathrm{T}}\boldsymbol{\varepsilon}_k$, which gives the virtual work done by the residual forces $\boldsymbol{\varepsilon}_k$ acting through virtual displacements $\tilde{\mathbf{u}}_k$ consistent with the two-component representation in Eq. (18). The energy associated with the error $\boldsymbol{\varepsilon}_k$ can then be minimized by requiring the virtual work $\tilde{\mathbf{u}}_k^{\mathrm{T}}\boldsymbol{\varepsilon}_k$ to vanish for any value of α_k, which yields the following orthogonality conditions:

$$\mathbf{u}_{0k}^{\mathrm{T}}\boldsymbol{\varepsilon}_k = 0, \qquad \mathbf{u}_{\infty k}^{\mathrm{T}}\boldsymbol{\varepsilon}_k = 0 \tag{20}$$

Combined with Eq. (19), these conditions yield the following equations:

$$\mathbf{u}_{0k}^{\mathrm{T}}(\mathbf{K} + \mathrm{i}\omega_k \mathbf{C} - \omega_k^2 \mathbf{M})\mathbf{u}_{0k} + \alpha_k \mathbf{u}_{0k}^{\mathrm{T}}(\mathbf{K} - \omega_k^2 \mathbf{M})\mathbf{u}_{\infty k} = 0 \tag{21}$$

$$\mathbf{u}_{\infty k}^{\mathrm{T}}(\mathbf{K} - \omega_k^2 \mathbf{M})\mathbf{u}_{0k} + \alpha_k \mathbf{u}_{\infty k}^{\mathrm{T}}(\mathbf{K} - \omega_k^2 \mathbf{M})\mathbf{u}_{\infty k} = 0 \tag{22}$$

The following relation between the mixed products, obtained by multiplication of the undamped eigenproblem (8) with $\mathbf{u}_{\infty k}^{\mathrm{T}}$, allows simplification of Eqs. (21) and (22):

$$\mathbf{u}_{\infty k}^{\mathrm{T}}\mathbf{K}\mathbf{u}_{0k} = \omega_{0k}^2 \mathbf{u}_{\infty k}^{\mathrm{T}}\mathbf{M}\mathbf{u}_{0k} \tag{23}$$

Making use of Eq. (23), taking advantage of the normalization of $\mathbf{u}_{0k}$ and $\mathbf{u}_{\infty k}$ according to Eqs. (9) and (16), and assuming symmetry of $\mathbf{M}$ and $\mathbf{K}$, the orthogonality conditions (21) and (22) become

$$(\omega_k^2 - \omega_{0k}^2)(1 + \alpha_k \mathbf{u}_{\infty k}^{\mathrm{T}}\mathbf{M}\mathbf{u}_{0k}) = \mathrm{i}\omega_k \mathbf{u}_{0k}^{\mathrm{T}}\mathbf{C}\mathbf{u}_{0k} \tag{24}$$

$$(\omega_k^2 - \omega_{0k}^2)\mathbf{u}_{\infty k}^{\mathrm{T}}\mathbf{M}\mathbf{u}_{0k} = \alpha_k(\omega_{\infty k}^2 - \omega_k^2) \tag{25}$$

Elimination of the mode shape coefficient α_k from Eqs. (24) and (25) gives the following equation for the complex eigenfrequency ω_k:

$$(\omega_k^2 - \omega_{0k}^2)\left[1 + \frac{\omega_k^2 - \omega_{0k}^2}{\omega_{\infty k}^2 - \omega_k^2}(\mathbf{u}_{\infty k}^{\mathrm{T}}\mathbf{M}\mathbf{u}_{0k})^2\right] = \mathrm{i}\omega_k \mathbf{u}_{0k}^{\mathrm{T}}\mathbf{C}\mathbf{u}_{0k} \tag{26}$$

while α_k is given by

$$\alpha_k = \frac{\omega_k^2 - \omega_{0k}^2}{\omega_{\infty k}^2 - \omega_k^2}\,\mathbf{u}_{\infty k}^{\mathrm{T}}\mathbf{M}\mathbf{u}_{0k} \tag{27}$$

Multiplication of Eq. (26) by $(\omega_{\infty k}^2 - \omega_k^2)$ and regrouping yields the following quartic equation in ω_k:

$$(\omega_k^2 - \omega_{0k}^2)[\omega_{\infty k}^2 - \omega_{0k}^2 - (\omega_k^2 - \omega_{0k}^2)(1 - (\mathbf{u}_{\infty k}^{\mathrm{T}}\mathbf{M}\mathbf{u}_{0k})^2)] = \mathrm{i}\omega_k \mathbf{u}_{0k}^{\mathrm{T}}\mathbf{C}\mathbf{u}_{0k}(\omega_{\infty k}^2 - \omega_k^2) \tag{28}$$

The product $\mathbf{u}_{0k}^{\mathrm{T}}\mathbf{C}\mathbf{u}_{0k}$ on the right of Eq. (28) is a measure of the dissipation in the kth undamped mode shape, and with the special form of the damping matrix in Eq. (5), this product can be expanded as

$$\mathbf{u}_{0k}^{\mathrm{T}}\mathbf{C}\mathbf{u}_{0k} = \sum_{j=1}^{r} c_j \gamma_{kj}^2 \tag{29}$$

where γ_{kj} denotes the differential displacement of the kth undamped mode shape across the jth damper:

$$\gamma_{kj} = \mathbf{w}_j^{\mathrm{T}}\mathbf{u}_{0k} \tag{30}$$

It is evident by inspection that Eq. (28) yields the solution $\omega_k^2 = \omega_{0k}^2$ when $\mathbf{u}_{0k}^{\mathrm{T}}\mathbf{C}\mathbf{u}_{0k} = 0$, and that it yields the solution $\omega_k^2 = \omega_{\infty k}^2$ when $\mathbf{u}_{0k}^{\mathrm{T}}\mathbf{C}\mathbf{u}_{0k} \to \infty$, corresponding to locking of the dampers. For finite values of $\mathbf{u}_{0k}^{\mathrm{T}}\mathbf{C}\mathbf{u}_{0k}$, Eq. (28) represents an interpolation between these limiting eigensolutions. Eq. (28) can be rearranged into a form suitable for iterative solution by collecting terms with ω_k^2 and dividing by the resulting factor, which yields

$$\omega_k^2 \simeq \frac{\omega_{0k}^2 + \mathrm{i}\omega_{\infty k}^2 \left[\dfrac{\omega_k \mathbf{u}_{0k}^{\mathrm{T}}\mathbf{C}\mathbf{u}_{0k}}{\omega_{\infty k}^2 - \omega_{0k}^2 - (\omega_k^2 - \omega_{0k}^2)(1 - (\mathbf{u}_{\infty k}^{\mathrm{T}}\mathbf{M}\mathbf{u}_{0k})^2)}\right]}{1 + \mathrm{i}\left[\dfrac{\omega_k \mathbf{u}_{0k}^{\mathrm{T}}\mathbf{C}\mathbf{u}_{0k}}{\omega_{\infty k}^2 - \omega_{0k}^2 - (\omega_k^2 - \omega_{0k}^2)(1 - (\mathbf{u}_{\infty k}^{\mathrm{T}}\mathbf{M}\mathbf{u}_{0k})^2)}\right]} \tag{31}$$

where the bracketed term in the denominator is the same as that in the numerator. Eq. (31) can be solved iteratively for ω_k by substituting the current estimate of ω_k into the right-hand side and taking the square root to obtain an improved estimate. The undamped eigenfrequency ω_{0k} can be used as the initial estimate of ω_k, and iteration can be continued until satisfactory convergence in ω_k is achieved. Adding and subtracting in the numerator allows elimination of the constant term ω_{0k}^2, and after rearrangement, Eq. (31) can be written in the following nondimensional form, which is also suitable for iterative solution:

$$\frac{\omega_k^2 - \omega_{0k}^2}{\omega_{\infty k}^2 - \omega_{0k}^2} \simeq \frac{\mathrm{i}\left[\dfrac{\omega_k \mathbf{u}_{0k}^{\mathrm{T}}\mathbf{C}\mathbf{u}_{0k}}{\omega_{\infty k}^2 - \omega_{0k}^2}\right]}{1 - \dfrac{\omega_k^2 - \omega_{0k}^2}{\omega_{\infty k}^2 - \omega_{0k}^2}(1 - (\mathbf{u}_{\infty k}^{\mathrm{T}}\mathbf{M}\mathbf{u}_{0k})^2) + \mathrm{i}\left[\dfrac{\omega_k \mathbf{u}_{0k}^{\mathrm{T}}\mathbf{C}\mathbf{u}_{0k}}{\omega_{\infty k}^2 - \omega_{0k}^2}\right]} \tag{32}$$

Once ω_k has been computed from Eq. (31) or (32), the corresponding value of α_k can be evaluated directly from Eq. (27).

4. Linearized explicit approximations

The accuracy of the assumed representation for the damped mode shape (18) depends on the closeness of the limiting eigensolutions, or equivalently, on the smallness of the perturbations in the eigenfrequencies and mode shapes induced by locking of the dampers. Formally introducing an assumption of small perturbations leads to approximations that allow substantial simplification of Eqs. (27) and (28), yielding simple, explicit approximations for the eigenfrequency ω_k and the mode shape coefficient α_k. While accuracy is sacrificed through the introduction of these additional approximations, the simplicity of the resulting explicit form affords important insights into the influence of the dampers on the eigenfrequencies and mode shapes.

4.1. Assumption of small perturbations

Following Krenk and Nielsen [14], it is convenient to introduce the notation $\Delta\omega_k$ to denote the complex-valued perturbation of the kth eigenfrequency produced by the dampers:

$$\Delta\omega_k = \omega_k - \omega_{0k}, \qquad \Delta\omega_{\infty k} = \omega_{\infty k} - \omega_{0k} \tag{33}$$

where $\Delta\omega_{\infty k}$ denotes the real-valued shift in the kth eigenfrequency produced by locking of the r dampers. It follows from Rayleigh's theorem on constraints (see e.g. Ref. [8]) that $\omega_{\infty k} \geqslant \omega_{0k}$, and consequently $\Delta\omega_{\infty k} \geqslant 0$. The assumption of small perturbations of the kth eigenfrequency can then be expressed as $\Delta\omega_{\infty k}/\omega_{0k} \ll 1$, which also insures that $|\Delta\omega_k|/\omega_{0k} \ll 1$. Under these restrictions, the following approximations can be introduced, which will prove useful subsequently in simplifying Eqs. (27) and (28) for α_k and ω_k, respectively:

$$\omega_k^2 - \omega_{0k}^2 \simeq \Delta\omega_k(2\omega_{0k}), \qquad \omega_{\infty k}^2 - \omega_{0k}^2 \simeq \Delta\omega_{\infty k}(2\omega_{0k}) \tag{34}$$

In a manner similar to Eq. (33), the real-valued perturbation of the kth mode shape produced by locking of the r dampers is denoted

$$\Delta\mathbf{u}_{\infty k} = \mathbf{u}_{\infty k} - \mathbf{u}_{0k} \tag{35}$$

The vectors $\mathbf{u}_{0k}$ and $\mathbf{u}_{\infty k}$ have unit norm with respect to $\mathbf{M}$ according to Eqs. (9) and (16), and the assumption that the perturbation $\Delta\mathbf{u}_{\infty k}$ is small with respect to $\mathbf{u}_{0k}$ can then be expressed in a consistent manner by requiring its norm with respect to $\mathbf{M}$ to be much less than unity, $\Delta\mathbf{u}_{\infty k}^{\mathrm{T}}\mathbf{M}\Delta\mathbf{u}_{\infty k} \ll 1$. Under this assumption, a simplifying approximation can be introduced for the mixed product $\mathbf{u}_{\infty k}^{\mathrm{T}}\mathbf{M}\mathbf{u}_{0k}$, which appears in Eqs. (27) and (32) for α_k and ω_k, respectively. By forming the product $\Delta\mathbf{u}_{\infty k}^{\mathrm{T}}\mathbf{M}\Delta\mathbf{u}_{\infty k}$, with $\Delta\mathbf{u}_{\infty k}$ given by Eq. (35) and $\mathbf{M}$ symmetric, it can be shown that $\mathbf{u}_{\infty k}^{\mathrm{T}}\mathbf{M}\mathbf{u}_{0k}$ is given by

$$\mathbf{u}_{\infty k}^{\mathrm{T}}\mathbf{M}\mathbf{u}_{0k} = 1 - \tfrac{1}{2}\Delta\mathbf{u}_{\infty k}^{\mathrm{T}}\mathbf{M}\Delta\mathbf{u}_{\infty k} \tag{36}$$

Under the small-perturbation assumption $\Delta\mathbf{u}_{\infty k}^{\mathrm{T}}\mathbf{M}\Delta\mathbf{u}_{\infty k} \ll 1$, the second term in Eq. (36) can be neglected, and the mixed product can be approximated as

$$\mathbf{u}_{\infty k}^{\mathrm{T}}\mathbf{M}\mathbf{u}_{0k} \simeq 1 \tag{37}$$

In the following sections, the approximations resulting from these small-perturbation assumptions will be used to develop explicit linearized approximations for the complex eigenfrequencies and mode shapes.

4.2. Complex eigenfrequencies

The quartic equation (28) for the complex eigenfrequency ω_k can be substantially simplified by introducing the approximation $\mathbf{u}_{\infty k}^{\mathrm{T}}\mathbf{M}\mathbf{u}_{0k} \simeq 1$ from Eq. (37). This leads to cancellation within the square brackets in Eq. (28), which simplifies to the following cubic equation in ω_k:

$$(\omega_k^2 - \omega_{0k}^2)(\omega_{\infty k}^2 - \omega_{0k}^2) = \mathrm{i}\omega_k \mathbf{u}_{0k}^{\mathrm{T}}\mathbf{C}\mathbf{u}_{0k}(\omega_{\infty k}^2 - \omega_k^2) \tag{38}$$

Collecting terms with ω_k^2 and rearranging as in Eq. (32) gives the following equation:

$$\frac{\omega_k^2 - \omega_{0k}^2}{\omega_{\infty k}^2 - \omega_{0k}^2} \simeq \frac{\mathrm{i}[\omega_k \mathbf{u}_{0k}^{\mathrm{T}}\mathbf{C}\mathbf{u}_{0k}/(\omega_{\infty k}^2 - \omega_{0k}^2)]}{1 + \mathrm{i}[\omega_k \mathbf{u}_{0k}^{\mathrm{T}}\mathbf{C}\mathbf{u}_{0k}/(\omega_{\infty k}^2 - \omega_{0k}^2)]} \tag{39}$$

where the bracketed term in the denominator is the same as that in the numerator. This equation can be simplified to an explicit equation for the complex-valued frequency increment $\Delta\omega_k$ (33) by introducing the approximation $\omega_k = \omega_{0k}$ within the bracketed term and introducing the approximations from Eq. (34), which are based on the assumption that $\Delta\omega_{\infty k}/\omega_{0k} \ll 1$. The constant factor ω_{0k} appears in each of these approximations, and it then cancels within the quotients in Eq. (39) to give the following important result:

$$\frac{\Delta\omega_k}{\Delta\omega_{\infty k}} \simeq \frac{\mathrm{i}\eta_k}{1 + \mathrm{i}\eta_k} \tag{40}$$

In this equation η_k is a normalized viscous damping parameter defined as

$$\eta_k = \frac{\mathbf{u}_{0k}^{\mathrm{T}}\mathbf{C}\mathbf{u}_{0k}}{2\Delta\omega_{\infty k}} \tag{41}$$

The subscript k emphasizes that η_k is a mode-specific parameter, because for a given damping matrix $\mathbf{C}$, each mode k has, in general, a different value of the parameter η_k. According to Eq. (41) the influence of the particular mode enters through the undamped mode shape $\mathbf{u}_{0k}$ and through the difference $\Delta\omega_{\infty k}$ (33) between the limiting eigenfrequencies.

Eq. (40) has the same form as the asymptotic approximation originally obtained by Krenk [13] for a taut cable with a viscous damper near one end, and subsequently extended to a sagging cable [14], rotation dampers at the ends of a beam [12], and to a tensioned beam with a viscous damper [15]. Taking the real and imaginary parts of Eq. (40) gives

$$\mathrm{Re}[\Delta\omega_k] \simeq \Delta\omega_{\infty k}\frac{\eta_k^2}{1 + \eta_k^2}, \qquad \mathrm{Im}[\Delta\omega_k] \simeq \Delta\omega_{\infty k}\frac{\eta_k}{1 + \eta_k^2} \tag{42}$$

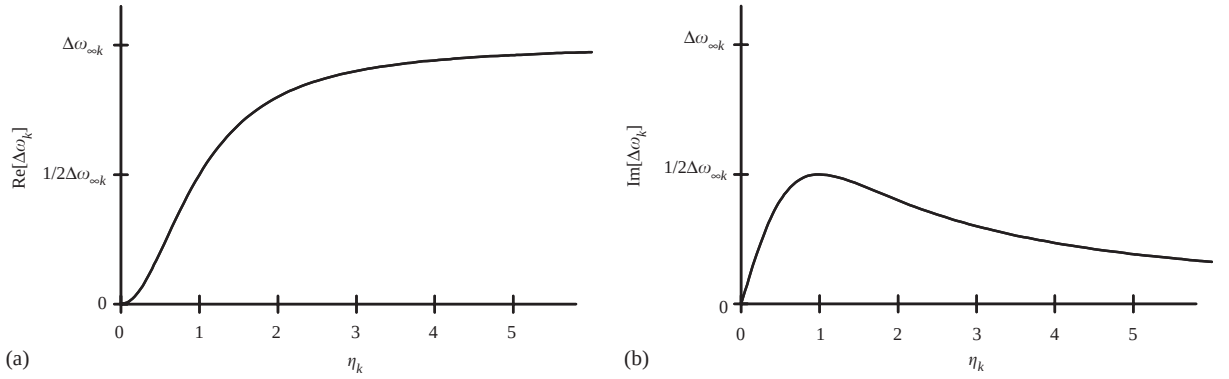

Fig. 3. Complex-valued frequency increment $\Delta\omega$: (a) real part; (b) imaginary part.

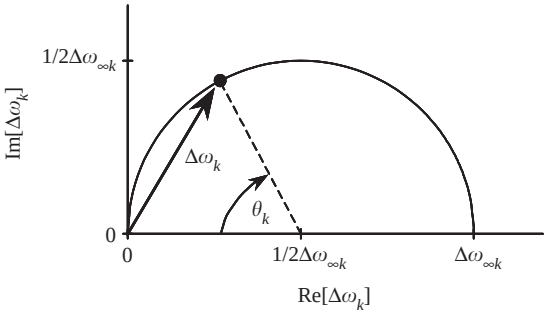

Fig. 4. Semi-circular locus of $\Delta\omega_k$ in complex plane.

These approximate relations are plotted in Fig. 3. The real part $\mathrm{Re}[\Delta\omega_k]$, plotted in Fig. 3(a), gives the shift in oscillation frequency, which increases monotonically with η_k and approaches $\Delta\omega_{\infty k}$ as η_k becomes large and the dampers approach locking. The imaginary part $\mathrm{Im}[\Delta\omega_k]$, plotted in Fig. 3(b), gives the rate of decay of free vibration, which determines the damping in the system. In contrast with $\mathrm{Re}[\Delta\omega_k]$, the imaginary part $\mathrm{Im}[\Delta\omega_k]$ does not increase monotonically, but takes on a maximum value of $\frac{1}{2}\Delta\omega_{\infty k}$ when $\eta_k = 1$, and tends to zero as η_k becomes large and the dampers approach locking. An optimal tuning of the dampers for mode k can be defined as that for which the decay rate $\mathrm{Im}[\Delta\omega_k]$ is maximized, corresponding to $\eta_k^{\mathrm{opt}} = 1$. It is noted that the curve for the imaginary part in Fig. 1(b) has the same form as the "universal estimation curve" identified numerically by Pacheco et al. [17] for a taut cable with viscous damper.

As discussed by Krenk and Nielsen [14], the form of Eq. (42) implies that the complex frequency increment $\Delta\omega_k$ traces a semi-circle in the complex plane with diameter $\Delta\omega_{\infty k}$. This semi-circle, depicted in Fig. 4, is conveniently parameterized as follows by an angle θ_k, where the subscript k emphasizes that θ_k is a mode-specific parameter, like η_k (41):

$$\mathrm{Re}[\Delta\omega_k] \simeq \tfrac{1}{2}\Delta\omega_{\infty k}(1-\cos\theta_k), \qquad \mathrm{Im}[\Delta\omega_k] \simeq \tfrac{1}{2}\Delta\omega_{\infty k}\sin\theta_k, \quad 0 \leqslant \theta_k < \pi \tag{43}$$

Because each mode has, in general, a different value of η_k, each mode occupies a different position on the semi-circle of Fig. 4, given by θ_k. Using Eq. (42), the nondimensional viscous damping

parameter η_k can be expressed as follows:

$$\eta_k \simeq \frac{\mathrm{Re}[\Delta\omega_k]}{\mathrm{Im}[\Delta\omega_k]} \tag{44}$$

Substituting Eq. (43) into Eq. (44) then gives the following expression relating η_k and θ_k:

$$\eta_k \simeq \tan\left(\tfrac{1}{2}\theta_k\right) \tag{45}$$

Eq. (45) shows that the semi-circle of Fig. 4 is traced in a clockwise sense with increasing η_k, since $\theta_k = 0$ when $\eta_k = 0$ and $\theta_k \to \pi$ as $\eta_k \to \infty$.

It is interesting to consider the form of the explicit approximation (40) for small values of η_k, corresponding to solutions near the undamped limit. With the restriction $\eta_k \ll 1$, Eq. (40) simplifies to $\Delta\omega_k \simeq \mathrm{i}\Delta\omega_{\infty k}\eta_k$. Substitution of the definition of η_k (41) into this relation then allows cancellation of the factor $\Delta\omega_{\infty k}$ to give

$$\Delta\omega_k \simeq \mathrm{i}\,\tfrac{1}{2}\mathbf{u}_{0k}^{\mathrm{T}}\mathbf{C}\mathbf{u}_{0k} \tag{46}$$

The restriction $\eta_k \ll 1$ used to obtain Eq. (46) can be expressed in the following alternative form using the definition of η_k in Eq. (41):

$$\tfrac{1}{2}\mathbf{u}_{0k}^{\mathrm{T}}\mathbf{C}\mathbf{u}_{0k} \ll \Delta\omega_{\infty k} \tag{47}$$

It is noted that the approximation in Eq. (46) is equivalent the result that is obtained through the assumption of light damping (see e.g. Refs. [8,9]). According to Eq. (46), the real part of the frequency increment is approximately zero, $\mathrm{Re}[\Delta\omega_k] \simeq 0$, while the imaginary part $\mathrm{Im}[\Delta\omega_k]$ increases approximately linearly with $\mathbf{u}_{0k}^{\mathrm{T}}\mathbf{C}\mathbf{u}_{0k}$, where $\mathbf{u}_{0k}^{\mathrm{T}}\mathbf{C}\mathbf{u}_{0k}$ represents the dissipation in the undamped mode shape. This approximation corresponds to the leftmost portion of the curves in Fig. 3, and the light damping approximation is clearly unable to capture the optimal portion of the curves and the transition to locking for large η_k.

4.3. Complex mode shapes

In the assumed form of approximation for the kth complex mode shape in Eq. (18), a single coefficient α_k is used to enforce a smooth transition between the limiting mode shapes, $\mathbf{u}_{0k}$ and $\mathbf{u}_{\infty k}$. As discussed previously, implicit in this representation is an assumption of proportionality among the r damper coefficients, such that locking of the dampers occurs uniformly. In the following section, approximate conditions on the relative sizing of dampers are obtained for which this assumption is justified. In cases where the assumed form (18) is appropriate, consideration of the complex-valued coefficient α_k affords insight into the nature of the complex mode shapes, as it represents the relative magnitude and phasing of the two components, $\mathbf{u}_{0k}$ and $\mathbf{u}_{\infty k}$.

An expression for α_k was previously obtained in Eq. (27), and introduction of the small-perturbation approximation $\mathbf{u}_{\infty k}^{\mathrm{T}}\mathbf{M}\mathbf{u}_{0k} \simeq 1$ (37) into this expression gives

$$\alpha_k \simeq \frac{\omega_k^2 - \omega_{0k}^2}{\omega_{\infty k}^2 - \omega_k^2} \tag{48}$$

This equation can be simplified by introducing the approximations from Eq. (34), which are based on the assumption that $\Delta\omega_{\infty k}/\omega_{0k} \ll 1$. The constant factor ω_{0k} from these approximations cancels

within the quotient in Eq. (48), to give the simplified approximation

$$\alpha_k \simeq \frac{\Delta\omega_k}{\Delta\omega_{\infty k} - \Delta\omega_k} \tag{49}$$

Substituting the explicit approximation for $\Delta\omega_k$ in Eq. (40) into Eq. (49) then shows that α_k is related to the normalized viscous damping parameter η_k as follows:

$$\alpha_k \simeq \mathrm{i}\eta_k \tag{50}$$

The approximate representation of the complex mode shape (18) can then be expressed as

$$\tilde{\mathbf{u}}_k = \mathbf{u}_{0k} + \mathrm{i}\eta_k \mathbf{u}_{\infty k} \tag{51}$$

The magnitude of $\tilde{\mathbf{u}}_k$ in Eq. (51) grows without bound as $\eta_k \to \infty$, and it is convenient to renormalize $\tilde{\mathbf{u}}_k$ to remain bounded. This can be accomplished using the angle θ_k, which defines the position on the semi-circle of Fig. 4 and is related to η_k by $\eta_k \simeq \tan(\frac{1}{2}\theta_k)$ according to Eq. (45). Substituting this relation into Eq. (51) and renormalizing through multiplication by $\cos(\frac{1}{2}\theta_k)$ yields the following alternative expression for $\tilde{\mathbf{u}}_k$:

$$\tilde{\mathbf{u}}_k = \cos(\tfrac{1}{2}\theta_k)\mathbf{u}_{0k} + \mathrm{i}\,\sin(\tfrac{1}{2}\theta_k)\mathbf{u}_{\infty k} \tag{52}$$

It is evident from the expressions in Eqs. (51) and (52) that $\tilde{\mathbf{u}}_k$ reduces to $\mathbf{u}_{0k}$ in the undamped limit when $\eta_k = 0$ and $\theta_k = 0$, and reduces to $\mathbf{u}_{\infty k}$ in the constrained limit when $\eta_k \to \infty$ and $\theta_k \to \pi$. For intermediate values of η_k and θ_k, both components contribute to the complex mode shape, with the contribution of $\mathbf{u}_{0k}$ purely real and the contribution of $\mathbf{u}_{\infty k}$ purely imaginary. At optimal damping ($\eta_k = 1$ and $\theta_k = \pi/2$) the two components contribute with equal magnitude.

The evolution in time of the displaced profile associated with $\tilde{\mathbf{u}}_k$ is given by $\mathbf{q} = \mathrm{Re}[\tilde{\mathbf{u}}_k \exp(\mathrm{i}\omega_k t)]$, according to the assumed expression for the generalized displacements in Eq. (2). Introducing Eq. (51) into this expression gives the following expression for the generalized displacements as a function of time:

$$\mathbf{q} = \exp(-\omega_k^I t)[\mathbf{u}_{0k}\,\cos(\omega_k^R t) - \eta_k \mathbf{u}_{\infty k}\,\sin(\omega_k^R t)] \tag{53}$$

In this expression, the notation $\omega_k^R = \mathrm{Re}[\omega_k]$ and $\omega_k^I = \mathrm{Im}[\omega_k]$ has been introduced for convenience. The exponential factor in Eq. (53) gives the decay resulting from dissipation in the dampers, while the expression in brackets gives the oscillation of the displaced profile. When $\eta_k = 0$, it follows that $\omega_k^I = 0$ and $\omega_k^R = \omega_{0k}$, and Eq. (53) expresses a nondecaying synchronous oscillation of the whole system in the real-valued undamped mode shape $\mathbf{u}_{0k}$. When $\eta_k \to \infty$, it follows that $\omega_k^I = 0$ and $\omega_k^R = \omega_{\infty k}$, and Eq. (53) expresses a nondecaying synchronous oscillation in the real-valued constrained mode shape $\mathbf{u}_{\infty k}$.

For finite η_k, Eq. (53) shows that both components contribute to the displaced profile, with $\mathbf{u}_{\infty k}$ leading $\mathbf{u}_{0k}$ in phase by 90°, and thus the decaying oscillation of the system is no longer synchronous. At instants when $\sin(\omega_k^R t) = 0$, the displaced profile is given by the undamped mode shape $\mathbf{u}_{0k}$, and one quarter period later, at instants when $\cos(\omega_k^R t) = 0$, the displaced profile is given by the constrained mode shape $\mathbf{u}_{\infty k}$. When the displacements of the undamped component $\mathbf{u}_{0k}$ reach their peak values, the velocities of the undamped component vanish, and thus there are no damping forces at this instant. One quarter-period later, when the displacements of the undamped component are very nearly zero, the velocities of the undamped component reach their peak values, and the damper forces also reach their peak values at this instant. These observations

illustrate that the generalized displacements given by Eq. (53) correspond to all damping forces having the same phasing. As discussed previously, such an assumption of uniform phasing in the damping forces is implicit in the assumed representation for the mode shape in Eq. (18), and the validity of this assumption depends on the relative sizing of the dampers, which is discussed in the following section.

4.4. Sizing of dampers

According to the approximations in Eqs. (40) and (51), the influence of the r dampers on the kth eigenfrequency and mode shape depends on the single parameter η_k, defined in Eq. (41). The product $\mathbf{u}_{0k}^{\mathrm{T}}\mathbf{C}\mathbf{u}_{0k}$ in Eq. (41) can be expanded as in Eq. (29) to give the following expression for η_k in terms of the r viscous coefficients c_j:

$$\eta_k = \tfrac{1}{2}\sum_{j=1}^{r} c_j\gamma_{kj}^2/\Delta\omega_{\infty k} \tag{54}$$

where γ_{kj} denotes the differential displacement of the kth undamped mode shape across the jth damper, defined in Eq. (30). In the case of a single damper ($r = 1$), the summation contains only one term, and Eq. (54) can be solved for the damper coefficient to give

$$c = 2\eta_k\Delta\omega_{\infty k}/\gamma_k^2 \tag{55}$$

in which the j subscripts have been dropped for this case of a single damper. Eq. (55) gives the value of the viscous coefficient necessary to achieve a desired value of the parameter η_k; optimal damping in mode k, for example, corresponds to $\eta_k = 1$. In the case of multiple dampers ($r>1$), there generally exist multiple combinations of the viscous coefficients c_j corresponding to any given value of η_k. In contrast with the single damper, Eq. (54) is then insufficient to uniquely specify the r damper coefficients corresponding to a desired value of η_k, and additional constraints on the relative sizing of the dampers are required.

As mentioned previously, implicit in the assumed two-component representation of the mode shape in Eq. (18) is an assumption that the damper coefficients are scaled in a proportionate manner such that the dampers lock uniformly as their strength is increased. It was also noted previously that this type of proportionate scaling is often desirable in order to improve the efficiency of the dampers, as is observed subsequently in an example. The form of the implicitly assumed proportionality among the damper coefficients is investigated in this section by identifying the relative scaling that minimizes the error resulting from the assumed mode shape in Eq. (18). The conditions thus derived provide the additional constraints necessary to uniquely specify each of the r damper coefficients to achieve a desired value of the parameter η_k.

Eq. (19) gives the error in the force balance resulting from the assumed form of the mode shape in Eq. (18), and this error can be expressed in the following alternative form by introducing the vector $\mathbf{R}_k$ (12) of reaction forces associated with the kth mode of the constrained system:

$$\boldsymbol{\varepsilon}_k = [\mathrm{i}\omega_k\mathbf{C} - (\omega_k^2 - \omega_{0k}^2)\mathbf{M}]\mathbf{u}_{0k} + \alpha_k[(\omega_{\infty k}^2 - \omega_k^2)\mathbf{M}\mathbf{u}_{\infty k} - \mathbf{R}_k] \tag{56}$$

in which the substitution $\mathbf{K}\mathbf{u}_{0k} = \omega_{0k}^2\mathbf{M}\mathbf{u}_{0k}$ from the undamped eigenvalue problem (8) has also been introduced. The terms involving $\mathbf{M}$ can be combined by introducing the approximation for

α_k in Eq. (48) to give

$$\boldsymbol{\varepsilon}_k \simeq (\omega_k^2 - \omega_{0k}^2)\mathbf{M}\Delta\mathbf{u}_{\infty k} + \mathrm{i}\omega_k \mathbf{C}\mathbf{u}_{0k} - \alpha_k \mathbf{R}_k \tag{57}$$

where $\Delta\mathbf{u}_{\infty k}$ is defined in Eq. (35). Introducing the approximation $\omega_k^2 - \omega_{0k}^2 \simeq \Delta\omega_k(2\omega_{0k})$ from Eq. (34), the error in force can be written as

$$\boldsymbol{\varepsilon}_k \simeq (2\omega_{0k})\Delta\omega_k \mathbf{M}\Delta\mathbf{u}_{\infty k} + \mathrm{i}\omega_k \mathbf{C}\mathbf{u}_{0k} - \alpha_k \mathbf{R}_k \tag{58}$$

Because both $\Delta\omega_k$ and $\Delta\mathbf{u}_{\infty k}$ are assumed small, the first term in Eq. (58) is of higher order and is neglected. Requiring the remaining terms to cancel then gives

$$\mathrm{i}\omega_k \mathbf{C}\mathbf{u}_{0k} = \alpha_k \mathbf{R}_k \tag{59}$$

This equation corresponds to the requirement that the damper forces are equivalent to the reaction forces necessary to equilibrate vibrations in the kth constrained mode, scaled by the factor α_k. The damping forces on the left side of Eq. (59) depend on the first component $\mathbf{u}_{0k}$ of the assumed mode shape (18), while the reaction forces on the right depend on the second component $\alpha_k \mathbf{u}_{\infty k}$, since $\mathbf{R}_k$ depends on $\mathbf{u}_{\infty k}$ according to Eq. (12). Expanding the damping matrix $\mathbf{C}$ and the reaction force vector $\mathbf{R}_k$ using their known forms in Eqs. (5) and (13), the force balance in Eq. (59) becomes:

$$\omega_{0k} \sum_{j=1}^{r} (c_j \mathbf{w}_j \mathbf{w}_j^{\mathrm{T}})\mathbf{u}_{0k} = \eta_k \sum_{j=1}^{r} \rho_{kj} \mathbf{w}_j \tag{60}$$

in which the approximations $\omega_k \simeq \omega_{0k}$ and $\alpha_k \simeq \mathrm{i}\eta_k$ (50) have been introduced. Combining the summations then gives

$$\sum_{j=1}^{r} (\omega_{0k} c_j \gamma_{kj} - \eta_k \rho_{kj})\mathbf{w}_j = \mathbf{0} \tag{61}$$

where γ_{kj} is defined in Eq. (30). Provided that the dampers are not placed in a redundant manner, the r vectors $\mathbf{w}_j$ are linearly independent, and for Eq. (61) to be satisfied, the quantity in parenthesis must equal zero for each value of j, giving the following equations:

$$c_j = \frac{\eta_k}{\omega_{0k}} \frac{\rho_{kj}}{\gamma_{kj}}, \quad j = 1, \ldots, r \tag{62}$$

These equations uniquely specify the value of each of the r viscous damper coefficients corresponding to a desired value of the parameter η_k; optimal damping in mode k, for example, corresponds to $\eta_k = 1$. Eq. (62) implies a relative sizing among the r viscous coefficients that can be expressed with respect to a reference damper ($j = 1$) as follows:

$$\frac{c_j}{c_1} = \frac{\rho_{kj}}{\rho_{k1}} \frac{\gamma_{k1}}{\gamma_{kj}} \tag{63}$$

Eqs. (62) and (63) dictate that the coefficient of the jth damper should be sized in a manner that is proportional to the jth constraint force in the kth constrained eigenmode ρ_{kj}, and that is inversely proportional to the differential displacement across the jth damper in the kth undamped eigenmode γ_{kj}. Subject to the small-perturbation assumptions, this type of scaling insures uniform

locking of the r dampers in mode k, thus insuring the accuracy of the present approximate formulation.

4.5. Placement of dampers

The semi-circular form of Fig. 4, predicted by Eq. (40), indicates that the maximum damping that can be provided in a given mode is proportional to $\Delta\omega_{\infty k}$ (33), the difference between the limiting eigenfrequencies. Because this frequency difference is produced by locking of all the dampers, it is independent of the sizing of the dampers and depends only on their location. The optimal placement for added dampers can thus be determined independently of their sizing by identifying the attachment locations for which locking of the dampers produces the largest frequency shift. This frequency difference can be evaluated directly from Eq. (33) after solving the limiting eigenvalue problems (8) and (11). However, solving the constrained eigenvalue problem (11) for all possible damper locations could be tedious for a large structure with several added dampers, and thus it is helpful to consider the factors that influence $\Delta\omega_{\infty k}$. In this section, an approximate expression is obtained for $\Delta\omega_{\infty k}$ that provides guidance in determining the damper locations that maximize this frequency difference.

Premultiplication of the constrained eigenvalue problem (11) by $\mathbf{u}_{0k}^{\mathrm{T}}$, which is equivalent to the requirement of zero virtual work through virtual displacements corresponding to the undamped mode shape, gives the following equation:

$$\mathbf{u}_{0k}^{\mathrm{T}}\mathbf{K}\mathbf{u}_{\infty k} - \omega_{\infty k}^2\mathbf{u}_{0k}^{\mathrm{T}}\mathbf{M}\mathbf{u}_{\infty k} + \mathbf{u}_{0k}^{\mathrm{T}}\mathbf{R} = 0 \tag{64}$$

With the assumption of symmetric $\mathbf{M}$ and $\mathbf{K}$, the first two terms can be combined using Eq. (23) to give

$$(\omega_{\infty k}^2 - \omega_{0k}^2)\mathbf{u}_{\infty k}^{\mathrm{T}}\mathbf{M}\mathbf{u}_{0k} = \mathbf{u}_{0k}^{\mathrm{T}}\mathbf{R} \tag{65}$$

By expanding the vector of reaction forces $\mathbf{R}_k$ in terms of the r independent constraint forces ρ_{kj} using Eq. (13), Eq. (65) can be written as:

$$(\omega_{\infty k}^2 - \omega_{0k}^2)\mathbf{u}_{\infty k}^{\mathrm{T}}\mathbf{M}\mathbf{u}_{0k} = \sum_{j=1}^{r} \rho_{kj}\gamma_{kj} \tag{66}$$

where γ_{kj} (30) is the displacement across the jth damper in the kth undamped mode shape. No approximations have been introduced in obtaining Eq. (66), and consequently, this relation is exact. Introducing the small-perturbation approximations, $\omega_{\infty k}^2 - \omega_{0k}^2 \simeq \Delta\omega_{\infty k}(2\omega_{0k})$ (34) and $\mathbf{u}_{\infty}^{\mathrm{T}}\mathbf{M}\mathbf{u}_0 \simeq 1$ (37), Eq. (66) yields the following approximation for the frequency difference $\Delta\omega_{\infty k}$:

$$\Delta\omega_{\infty k} \simeq \sum_{j=1}^{r} \frac{\rho_{kj}\gamma_{kj}}{2\omega_{0k}} \tag{67}$$

This approximation is of limited use in actually estimating the frequency difference $\Delta\omega_{\infty k}$, because determination of the constraint forces ρ_{kj} requires solving the constrained eigenvalue problem (11), and if Eq. (11) is to be solved, the frequency difference $\Delta\omega_{\infty k}$ should be evaluated directly from Eq. (33) rather than using this approximation. However, Eq. (67) does clearly indicate that larger values of differential displacement γ_{kj} lead to larger values of $\Delta\omega_{\infty k}$. This

suggests that to maximize $\Delta\omega_{\infty k}$, the dampers should be placed so as to maximize the displacement across the dampers in the kth undamped mode shape. In this way, potentially effective locations for added dampers can be identified through consideration of the undamped mode shape alone.

5. Multi-story building example

The applicability of the foregoing approximate formulation and its use in determining the optimal placement and sizing of added dampers are now illustrated through numerical examples. A simplified multi-story shear-type building model is considered, as depicted in Fig. 1. This building model has uniform floor mass M and uniform interstory stiffness K. In the general case of n stories and r added dampers with viscous coefficients c_j, the quadratic eigenvalue problem (3) associated such a system can be written in nondimensional form as follows:

$$\left(\begin{bmatrix} 2 & -1 & & \\ -1 & 2 & -1 & \\ & & \ddots & \\ & & -1 & 1 \end{bmatrix} + \mathrm{i}\tilde{\omega}\sum_{j=1}^{r}\tilde{c}_j\mathbf{w}_j\mathbf{w}_j^{\mathrm{T}} - \tilde{\omega}^2\begin{bmatrix} 1 & & & \\ & 1 & & \\ & & \ddots & \\ & & & 1 \end{bmatrix}\right)\begin{Bmatrix} u_1 \\ u_2 \\ \vdots \\ u_n \end{Bmatrix} = \begin{Bmatrix} 0 \\ 0 \\ \vdots \\ 0 \end{Bmatrix} \tag{68}$$

where $\tilde{\omega} = \omega/\sqrt{K/M}$ is a nondimensional complex angular frequency, $\mathbf{u} = [u_1 \ \cdots \ u_n]^{\mathrm{T}}$ is the corresponding complex-valued vector of floor displacements, and the $\tilde{c}_j = c_j/\sqrt{KM}$ are nondimensional viscous coefficients. The $(n \times 1)$ vectors $\mathbf{w}_j$ represent the attachment positions of the dampers and have the forms illustrated in Eqs. (6) and (7) for the five-story building of Fig. 1. Only dampers that connect adjacent floors are considered in this example, and consequently, damping due to absolute motion, as in Eq. (6), can only be achieved for a damper attached between the ground and the first floor. Dampers attached at higher floors produce forces due to relative motion, as in Eq. (7). The undamped eigenfrequencies $\tilde{\omega}_{0k}$ and mode shapes $\mathbf{u}_{0k}$ can be readily evaluated from Eq. (68) by setting $\tilde{c}_j = 0$ for all j, and the constrained eigenfrequencies $\tilde{\omega}_{\infty k}$ and mode shapes $\mathbf{u}_{\infty k}$ can be evaluated by using a reduced set of generalized coordinates, as discussed previously and illustrated in Fig. 2(b). To facilitate numerical solution in the case of finite damping, Eq. (68) can be recast in state-space form as a linear eigenvalue problem (see e.g. Ref.[8]), and the nondimensional eigenvalues $\tilde{\omega}_k$ and corresponding eigenvectors $\mathbf{u}_k$ can then be computed using standard eigensolvers. In the following examples, a 10-story building ($n = 10$) is considered.

5.1. Single damper

In the case of a single damper, the index j in Eq. (68) is omitted, and the viscous coefficient is denoted c. The location of the inter-story damper can be represented by denoting the upper floor of attachment m, so that the differential displacement across the damper corresponds to the inter-story displacement between floors m and $(m-1)$. According to Eq. (30), the inter-story displacement across the damper in the kth undamped mode shape is then given by $\gamma_k = \mathbf{w}^{\mathrm{T}}\mathbf{u}_{0k}$,

Table 1
Influence of damper location m on perturbations of first-mode eigenfrequency and mode shape

m	1	2	4	7
γ_1	0.0650	0.0636	0.0565	0.0367
$\Delta\omega_{\infty 1}/\omega_{01}$	0.1050	0.1018	0.0787	0.0306
$\Delta\mathbf{u}_{\infty 1}^{\mathrm{T}}\mathbf{M}\Delta\mathbf{u}_{\infty 1}$	0.0108	0.0062	0.0027	0.0022

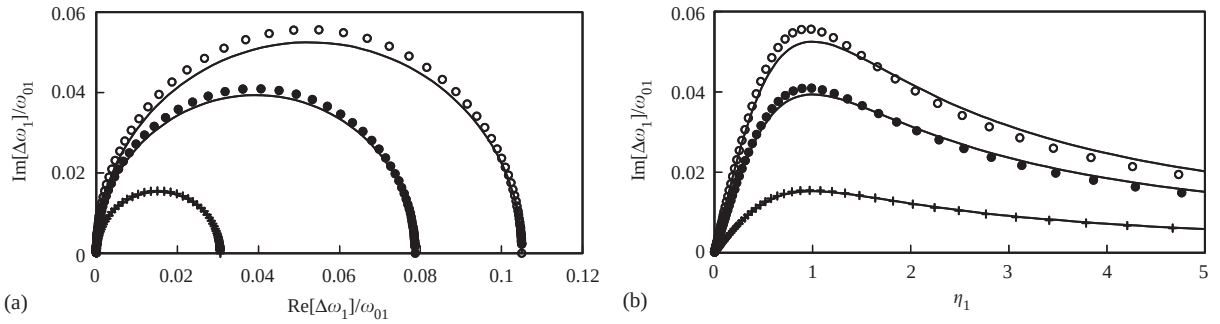

Fig. 5. First-mode frequency increment $\Delta\omega_1$ with varying damper location m. Explicit approximation, —-; $m = 1$, ○; $m = 4$, •; $m = 7$, +. (a) Locus in complex plane; (b) imaginary part.

which can be readily evaluated from the undamped mode shape $\mathbf{u}_{0k}$ for different damper locations by varying $\mathbf{w}$.

Eq. (67) suggests that to maximize $\Delta\omega_{\infty k}$ and thus to maximize the damping potential in mode k, the damper should be placed so as to maximize the inter-story displacement across the damper, γ_k. The first row of Table 1 presents values of interstory displacement γ_1 in the first undamped mode shape with varying damper location m, in which it is evident that the largest inter-story displacement occurs between the first floor and the ground level ($m = 1$). Normalized values of the first-mode frequency shift $\Delta\omega_{\infty 1}/\omega_{01}$ are presented in the second row of Table 1, and these values confirm that the largest shift in frequency is produced by the first-story damper location ($m = 1$). The values in the second row of Table 1 also enable a check on the appropriateness of the assumption of small perturbations in eigenfrequency for the first mode of this system with a single damper. These values show that the appropriateness of the assumption $\Delta\omega_{\infty 1}/\omega_{01} \ll 1$ improves with increasing m, while even for $m = 1$ the assumption is reasonable. Values of $\Delta\mathbf{u}_{\infty 1}^{\mathrm{T}}\mathbf{M}\Delta\mathbf{u}_{\infty 1}$ in the third row of Table 1 show that the assumption $\Delta\mathbf{u}_{\infty 1}^{\mathrm{T}}\mathbf{M}\Delta\mathbf{u}_{\infty 1} \ll 1$ of small perturbations in the first mode shape is also justified.

The validity of the small-perturbation assumptions implies that the linearized approximation (40) should give accurate estimates of the complex frequency increment $\Delta\omega_1$, and the plots of Fig. 5 show good agreement between the explicit approximation and the exact solutions for three different damper locations ($m = 1$, 4, and 7). Fig. 5(a) shows loci of the normalized frequency increment $\Delta\omega_1/\omega_{01}$ in the complex plane, as in Fig. 4, while Fig. 5(b) shows the normalized decay rate $\mathrm{Im}[\Delta\omega_1]/\omega_{01}$ against the normalized viscous damping parameter η_1, as in Fig. 3(b). For

Table 2
Deviations from explicit approximation in higher modes ($m = 1$)

k	1	2	3	4
$\Delta\omega_{\infty k}/\omega_{0k}$	0.1050	0.1032	0.0995	0.0939
$\Delta\mathbf{u}_{\infty k}^{\mathrm{T}}\mathbf{M}\Delta\mathbf{u}_{\infty k}$	0.0108	0.0762	0.2032	0.3845
$\mathrm{Im}[\Delta\omega_k^{\mathrm{opt}}]/\Delta\omega_{\infty k}$	0.5294	0.5499	0.5995	0.7127
η_k^{opt}	0.9433	0.9198	0.8750	0.8190

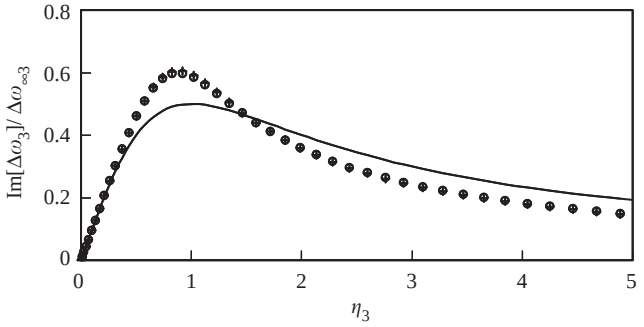

Fig. 6. Comparison of exact solution with iterative and explicit approximations ($m = 1$, mode 3). Exact, ○; iterative, +; explicit, —.

$m = 7$, the exact and approximate values are virtually indistinguishable, while deviations are more significant for $m = 1$, for which the maximum damping is achieved. These deviations of the exact values from the explicit approximation correspond to a slight increase in the maximum decay rate $\mathrm{Im}[\Delta\omega_1^{\mathrm{opt}}]/\omega_{01}$ and a slight decrease in the corresponding optimal value of the viscous damping parameter η_1^{opt}.

These deviations from the explicit approximation become more significant in the higher modes, as shown in Table 2 for a first-story damper location ($m = 1$). The first row of Table 2 shows that the normalized eigenfrequency perturbation $\Delta\omega_{\infty k}/\omega_{0k}$ actually decreases slightly with increasing mode number k, so that the assumption $\Delta\omega_{\infty k}/\omega_{0k} \ll 1$ remains reasonable in higher modes. (It is noted that while numerical values of $\Delta\omega_{\infty k}$ increase with mode number k, the undamped frequencies ω_{0k} increase more strongly with k for this system, leading to a slight decrease of the ratio $\Delta\omega_{\infty k}/\omega_{0k}$ with increasing k.) In contrast, the mode shape perturbation $\Delta\mathbf{u}_{\infty k}^{\mathrm{T}}\mathbf{M}\Delta\mathbf{u}_{\infty k}$ increases strongly with mode number, as shown in the second row of Table 2. This increase in $\Delta\mathbf{u}_{\infty k}^{\mathrm{T}}\mathbf{M}\Delta\mathbf{u}_{\infty k}$ renders the assumption $\Delta\mathbf{u}_{\infty k}^{\mathrm{T}}\mathbf{M}\Delta\mathbf{u}_{\infty k} \ll 1$ less appropriate, leading to increases of the maximum decay rate from the explicit approximation $\mathrm{Im}[\Delta\omega_k^{\mathrm{opt}}]/\Delta\omega_{\infty k} = 0.5$, as shown in the third row of Table 2, and to decreases of the corresponding optimal viscous damping parameter from the explicit approximation $\eta_k^{\mathrm{opt}} = 1$, as shown in the fourth row. Improved agreement with the exact values can be achieved by using the iterative solution (31) rather than the explicit approximation (40). This is illustrated in Fig. 6 for the third mode ($k = 3$) with a first-story damper ($m = 1$), in which the iterative and exact solutions are virtually indistinguishable.

Table 3
Influence of second damper location m_2 in first mode ($m_1 = 1$)

m_2	2	5	7	10
$\Delta\omega_{\infty 1}/\omega_{01}$	0.2347	0.1949	0.1500	0.1081
$\Delta\mathbf{u}_{\infty 1}^{\mathrm{T}}\mathbf{M}\Delta\mathbf{u}_{\infty 1}$	0.0426	0.0094	0.0080	0.0103
γ_{12}/γ_{11}	0.9777	0.7840	0.5649	0.1495
ρ_{12}/ρ_{11}	1.0000	0.8137	0.5867	0.1613
c_2/c_1	1.0228	1.0378	1.0386	1.0789

5.2. Two dampers

In the case of two dampers, the viscous coefficients are denoted c_1 and c_2, and the upper floors of attachment are denoted m_1 and m_2, where $m_1 \neq m_2$. A first-story location is considered for the first damper ($m_1 = 1$), at which a single damper is known to produce the greatest effect in the first mode, and different locations for the second damper are considered. Based on the first-mode inter-story displacements in Table 1, it would be expected that a location of $m_2 = 2$ for the second damper would produce the greatest effect, and this is confirmed by the value of the frequency shift $\Delta\omega_{\infty 1}$ in the first row of Table 3, which is highest for $m_2 = 2$ and decreases with increasing m_2. The norm of the mode shape perturbation $\Delta\mathbf{u}_{\infty 1}^{\mathrm{T}}\mathbf{M}\Delta\mathbf{u}_{\infty 1}$ in the second row of Table 3 is also highest for $m_2 = 2$, thus leading to improved accuracy in the explicit approximation but decreased damping for larger values of m_2.

In order to insure uniform action of the two dampers in the first mode and thus maximize the accuracy of the assumed mode shape (18), the viscous coefficients should be proportioned according to Eq. (63), which for the first mode gives $c_2/c_1 = (\rho_{12}/\rho_{11})(\gamma_{12}/\gamma_{11})^{-1}$. The third row of Table 3 shows the ratio of the inter-story displacements γ_{12}/γ_{11}, determined from the undamped mode shape $\mathbf{u}_{01}$, and the fourth row of Table 3 shows the ratio of the constraint forces ρ_{12}/ρ_{11}, determined from the constrained mode shape $\mathbf{u}_{\infty 1}$ using Eq. (14). The fifth row of Table 3 shows the resulting ratio of the damper coefficients c_2/c_1. It is observed that for this system with uniform floor mass and inter-story stiffness, the ratio c_2/c_1 is approximately unity and is fairly insensitive to the location m_2 of the second damper.

Each value of the ratio c_2/c_1 defines a locus of the frequency increment $\Delta\omega_1$ in the complex plane, which can be determined by increasing both c_1 and c_2 in Eq. (68) according to this fixed ratio and repeatedly solving for ω_1. In Fig. 7, the exact values of $\Delta\omega_1$, evaluated in this way, are compared with values corresponding to the explicit approximation (40) for three different locations of the second damper ($m_2 = 2$, 5, and 7, with $m_1 = 1$). The exact values for each damper location m_2 in Fig. 7 were computed with $c_2/c_1 = 1$, which corresponds very nearly to the proportional scaling given by Eq. (63), as shown in Table 3. Reasonable agreement is observed between the exact and approximate values with the dampers proportioned in this way. The discrepancies are most significant for $m_2 = 2$, for which the perturbations $\Delta\omega_{\infty 1}$ and $\Delta\mathbf{u}_{\infty 1}$ are largest, as shown in Table 3. As illustrated previously in Fig. 6, improved accuracy can be achieved by using the iterative solution (31) rather than the linearized approximation (40).

Fig. 8 shows a comparison of the approximate representation of the first mode shape, $\tilde{\mathbf{u}}_1 = \mathbf{u}_{01} + \alpha_1\mathbf{u}_{\infty 1}$ (18), with the exact mode shape $\mathbf{u}_1$ evaluated numerically from Eq. (68). This

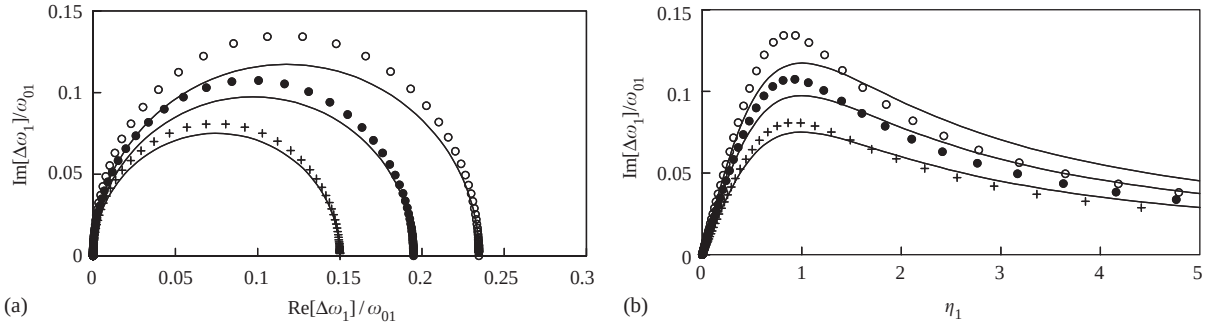

Fig. 7. First-mode frequency increment $\Delta\omega_1$ with two dampers ($m_1 = 1$, varying m_2, $c_2/c_1 = 1$). Explicit approximation, —; $m_2 = 1$, ○; $m_2 = 4$, •; $m_2 = 7$, +. (a) Locus in complex plane; (b) imaginary part.

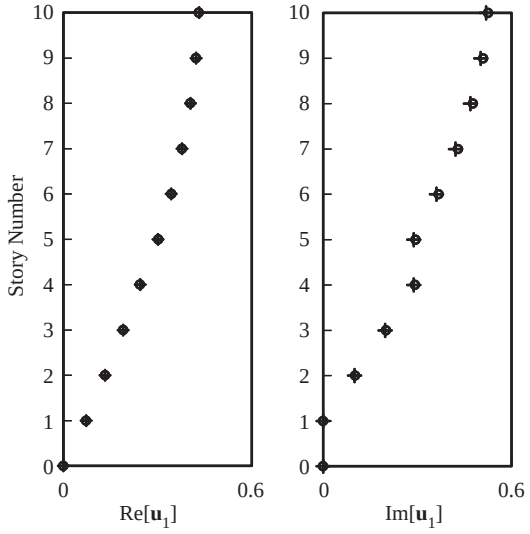

Fig. 8. Comparison of exact and approximate mode shapes near optimal damping ($\eta_1 = 1$, $m_1 = 1$, $m_2 = 5$, $c_2/c_1 = 1$, mode 1). Exact, ○; approximate, +.

comparison corresponds to $\eta_1 = 1$, near optimal damping in the first mode, with damper locations given by $m_1 = 1$ and $m_2 = 5$, and with the dampers proportioned according to $c_2/c_1 = 1$. To obtain the best possible accuracy in the approximate representation, the coefficient α_1 is evaluated from Eq. (27), in which no small-perturbation approximations have been introduced, and the approximate eigenfrequency ω_1 in this expression for α_1 is evaluated iteratively from Eq. (31). To facilitate comparison, both the exact and approximate mode shapes are normalized so that the displacement across the first damper is purely real, $\mathrm{Im}[\mathbf{w}_1^{\mathrm{T}}\mathbf{u}_1] = 0$, and so that the real part has unit norm with respect to $\mathbf{M}$, $\mathrm{Re}[\mathbf{u}_1^{\mathrm{T}}]\mathbf{M}\mathrm{Re}[\mathbf{u}_1] = 1$. The approximate mode shape is generally least accurate around optimal damping, since it reduces to the exact mode shape in the undamped and constrained limits. However, Fig. 8 shows excellent agreement between the exact and approximate

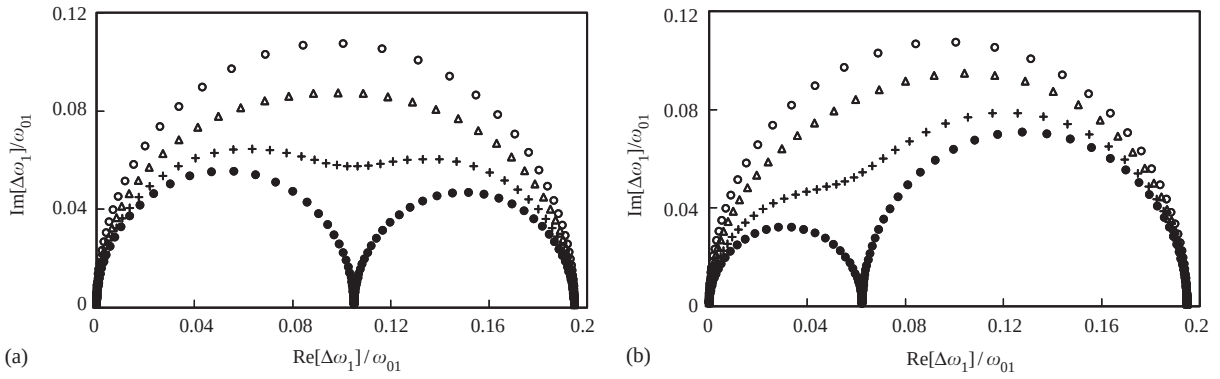

Fig. 9. Influence of damper proportioning, c_2/c_1 ($m_1 = 1, m_2 = 5$). (a) $c_2 \leqslant c_1$: $c_2/c_1 = 1$, ○; $c_2/c_1 = 0.3$, △; $c_2/c_1 = 0.1$, +; $c_2/c_1 \to 0$, •. (b) $c_1 \leqslant c_2$: $c_1/c_2 = 1$, ○; $c_1/c_2 = 0.3$, △; $c_1/c_2 = 0.1$, +; $c_1/c_2 \to 0$, •.

mode shapes, even in this case near optimal damping and with the moderately large value of the eigenfrequency perturbation $\Delta\omega_{\infty 1}$ shown in Table 3.

Fig. 9 shows the influence of the relative sizing of the dampers c_2/c_1 on the loci of $\Delta\omega_1$ in the complex plane, with damper locations given by $m_1 = 1$ and $m_2 = 5$. The loci in Fig. 9 are exact, and were evaluated numerically by increasing both c_1 and c_2 in Eq. (68) according to the specified ratio and repeatedly solving for ω_1. The loci in Fig. 9(a) correspond to $c_2/c_1 \leqslant 1$, where $c_2/c_1 = 1$ corresponds to proportional scaling, as specified by Eq. (63). In these cases, the first damper begins to lock before the second damper. The limiting curve labeled $c_2/c_1 \to 0$ corresponds to the case of first letting $c_1 \to \infty$ with $c_2 = 0$ and then letting $c_2 \to \infty$ while the first damper remains locked. In this limiting case, two local maxima of the decay rate $\mathrm{Im}[\Delta\omega_1]$ are observed, both of which are less than the maximum value of $\mathrm{Im}[\Delta\omega_1]$ in the case of proportional scaling, $c_2/c_1 = 1$. As c_2/c_1 decreases from the case of proportional scaling, the loci in Fig. 9(a) deviate from a nearly semi-circular form and tend towards the limiting curves associated with $c_2/c_1 \to 0$, thus resulting in decreased damping. Similar features are observed in Fig. 9(a), corresponding to $c_2/c_1 \geqslant 1$, for which the second damper begins to lock before the first. It is thus observed that the proportional scaling (63), which is implicit in the assumed representation of the mode shape (18) leads to the maximum efficiency in a given mode.

6. Conclusions

An approximate solution has been developed for the complex eigenfrequencies of a discrete system with several viscous dampers. The approximate solution is developed through an interpolation procedure, in which a given mode shape has been represented as a linear combination of the mode shapes corresponding to the two limiting eigenproblems: the undamped eigenproblem and the constrained eigenproblem in which each damper has been replaced with a rigid link. The requirement of zero virtual work through arbitrary virtual displacements consistent with this two-component representation yields approximations for the complex eigenfrequency and for the relative magnitude and phasing of the two components of the complex mode shape.

The validity of the two-component mode shape representation requires uniform locking of each damper in the system, as this approximation is unable to capture independent locking of a specific damper with other dampers remaining compliant. However, when the dampers are intended to work together to damp a particular mode, this condition of uniform locking is desirable, and explicit conditions have been obtained on the relative sizing of the dampers to insure such uniform locking. The advantage of the proposed approximation is that the efficiency and tuning of viscous dampers in a given mode can be investigated by solving only the two limiting eigenproblems, rather than repeatedly solving the complex eigenvalue problem of the damped system with different values of the viscous coefficients. A simple iterative procedure has been presented for efficient evaluation of the complex frequencies.

For cases in which the difference between the undamped and fully locked mode shapes is sufficiently small, an explicit approximation for the complex eigenfrequency has been obtained, having the same form as asymptotic approximations previously derived for cables and beams with a single concentrated damper near one end. This approximation indicates that as the strength of the dampers is increased, the complex eigenfrequency in a given mode traces a semi-circle in the complex plane, originating at the undamped eigenfrequency and terminating at the eigenfrequency of the constrained system with locked dampers. The maximum damping that can be added in a given mode is thus proportional to the shift in the eigenfrequency induced by locking of the dampers. This frequency shift has been shown to increase with the differential displacement across the damper in the undamped mode shape, indicating that to maximize damping in a given mode, the damper should be placed so as to maximize the displacement across the damper in that undamped mode shape. Application of this approximate formulation has been illustrated for a 10-story shear building with one or two added dampers. For this system, the explicit approximation has been shown to be fairly accurate, and improved accuracy can be achieved through an iterative scheme.

Acknowledgements

This work has been supported by the Danish Technical Research Council through the project "Damping Mechanisms in Dynamics of Structures and Materials".

Appendix A. Alternative derivation for single damper

In the case of a single damper, the approximate cubic equation (38) for the complex eigenfrequencies ω_k can be obtained in an alternative way using an exact analytical expression recently obtained by Gürgöze [16] for the characteristic equation of a discrete system with several added dampers. Gürgöze extended a result previously obtained by Cha and Wong [18] to obtain an expression for the characteristic equation as the determinant of a reduced-order matrix. The dimension of this reduced matrix is given by the number of added dampers rather than the number of degrees of freedom, while each term in the matrix contains a summation over all modes. In the case of a single added damper this matrix reduces to a single term, given in Eq. (18) in Ref. [16]. Neglecting inherent damping, this characteristic equation can be written as follows

using the present notation:

$$1 + \mathrm{i}c\omega \sum_{k=1}^{n} \frac{\gamma_k^2}{\omega_{0k}^2 - \omega^2} = 0 \tag{A.1}$$

where c is the viscous coefficient of the single damper, ω_{0k} denotes the kth undamped frequency, and γ_k denotes the differential displacement across the kth undamped mode shape. This differential displacement is defined in Eq. (30) as γ_{kj}, where the subscript j denotes the damper number, but in Eq. (A.1) the subscript j is omitted for this case of a single damper. The values of ω for which Eq. (A.1) is satisfied are the complex-valued eigenfrequencies ω_k of the damped system. To clarify the limit associated with $c \to \infty$, is it convenient to divide Eq. (A.1) by c, giving the following equation:

$$\frac{1}{c} + \mathrm{i}\omega \sum_{k=1}^{n} \frac{\gamma_k^2}{\omega_{0k}^2 - \omega^2} = 0 \tag{A.2}$$

Clearly the first term tends to zero as $c \to \infty$, so the summation in the second term must also tend to zero in this limit. The values of ω for which this summation vanishes are then the real-valued eigenfrequencies $\omega_{\infty k}$ of the system in which the damper has been replaced with a rigid link.

When a particular eigenfrequency ω_r is of interest, it is convenient to isolate the rth term of the summation in Eq. (A.2) as follows:

$$\sum_{k=1}^{n} \frac{\gamma_k^2}{\omega_{0k}^2 - \omega_r^2} = \frac{\gamma_r^2}{\omega_{0r}^2 - \omega_r^2} + \sum_{k \neq r}^{n} \frac{\gamma_k^2}{\omega_{0k}^2 - \omega_r^2} \tag{A.3}$$

As $c \to 0$, the rth eigenfrequency approaches its undamped value $\omega_r \to \omega_{0r}$, and in this limit the isolated term in Eq. (A.3) tends to infinity and the other terms in the summation become unimportant. As $c \to \infty$, it follows from Eq. (A.2) that the summation on the left-hand side of Eq. (A.3) tends to zero, which requires cancellation of the rth term with the remaining terms in the summation on the right-hand side of Eq. (A.3). In the limit as $c \to \infty$ and $\omega_r \to \omega_{\infty r}$, Eq. (A.3) can then be written as follows:

$$\sum_{k \neq r}^{n} \frac{\gamma_k^2}{\omega_{0k}^2 - \omega_{\infty r}^2} = \frac{\gamma_r^2}{\omega_{\infty r}^2 - \omega_{0r}^2} \tag{A.4}$$

Eq. (A.4) gives a simple single-term expression for the value of the summation on the right-hand side of Eq. (A.3) in the limit as $c \to \infty$ and $\omega_r \to \omega_{\infty r}$. Provided the limiting eigenfrequencies, ω_{0r} and $\omega_{\infty r}$, are fairly close to each other so that changes in ω_r are small, the value of the summation on the right hand of Eq. (A.3) is quite insensitive to changes in ω_r, and it can be approximated by its known value for $\omega_r \to \omega_{\infty r}$ in Eq. (A.4):

$$\sum_{k \neq r}^{n} \frac{\gamma_k^2}{\omega_{0k}^2 - \omega_r^2} \simeq \frac{\gamma_r^2}{\omega_{\infty r}^2 - \omega_{0r}^2} \tag{A.5}$$

Using this approximation, Eq. (A.3) becomes

$$\sum_{k=1}^{n} \frac{\gamma_k^2}{\omega_{0k}^2 - \omega_r^2} \simeq \gamma_r^2 \left(\frac{1}{\omega_{0r}^2 - \omega_r^2} + \frac{1}{\omega_{\infty r}^2 - \omega_{0r}^2} \right) \tag{A.6}$$

Combining the two terms on the right-hand side and substituting this approximation into Eq. (A.2) then gives

$$\frac{1}{c} + \mathrm{i}\omega_r \gamma_r^2 \frac{\omega_{\infty r}^2 - \omega_r^2}{(\omega_{0r}^2 - \omega_r^2)(\omega_{\infty r}^2 - \omega_{0r}^2)} \simeq 0 \tag{A.7}$$

which can be rearranged to yield

$$(\omega_r^2 - \omega_{0r}^2)(\omega_{\infty r}^2 - \omega_{0r}^2) \simeq \mathrm{i}\omega_r c \gamma_r^2 (\omega_{\infty r}^2 - \omega_r^2) \tag{A.8}$$

According to Eq. (29), $\mathbf{u}_{0r}^{\mathrm{T}} \mathbf{C} \mathbf{u}_{0r} = c\gamma_r^2$ in the case of a single damper, and thus Eq. (A.8) is equivalent to Eq. (38), apart from the use of the subscript r to denote the mode number, rather than k as in Eq. (38).

References

[1] E. Rasmussen, Dampers hold sway, *Civil Engineering Magazine* 67 (3) (1997) 40–43.
[2] T.T. Soong, G.F. Dargush, *Passive Energy Dissipation Systems in Structural Engineering*, Wiley, Chichester, 1997.
[3] R.D. Hanson, T.T. Soong, *Seismic Design with Supplemental Energy Dissipation Devices*, MNO-8, Earthquake Engineering Research Institute, Oakland, CA, 2001.
[4] J.A. Main, N.P. Jones, Evaluation of viscous dampers for stay-cable vibration mitigation, *Journal of Bridge Engineering* 6 (2001) 385–397.
[5] P. Dallard, A.J. Fitzpatrick, A. Flint, S. Le Bourva, A. Low, R.M. Ridsdill Smith, M. Willford, The London Millennium Footbridge, *The Structural Engineer* 79 (2001) 17–33.
[6] A. Preumont, *Vibration Control of Active Structures*, 2nd ed., Kluwer, Dordrecht, The Netherlands, 2002.
[7] T.K. Caughey, M.E.J. O'Kelly, Classical normal modes in damped linear dynamic systems, *Journal of Applied Mechanics* 32 (1965) 583–588.
[8] M. Géradin, D. Rixen, *Mechanical Vibrations*, 2nd ed., Wiley, Chichester, 1997.
[9] J. Woodhouse, Linear damping models for structural vibration, *Journal of Sound and Vibration* 215 (1998) 547–569.
[10] J.W.S. Rayleigh, *The Theory of Sound*, Vol. I, 1877, re-issued, Dover Publications, New York, 1945.
[11] K.A. Foss, Coordinates which uncouple the equations of motion of damped linear dynamic systems, *Journal of Applied Mechanics* 35 (1958) 361–367.
[12] S. Krenk, Complex modes and frequencies in damped structural vibrations, *Journal of Sound and Vibration* 270 (2004) 981–996.
[13] S. Krenk, Vibrations of a taut cable with an external damper, *Journal of Applied Mechanics* 67 (2000) 772–776.
[14] S. Krenk, S.R.K. Nielsen, Vibrations of a shallow cable with a viscous damper, *Proceedings of the Royal Society of London Series A* 458 (2002) 339–357.
[15] J.A. Main, N.P. Jones, Combined effects of flexural stiffness and axial tension on damper effectiveness in slender structures, *Proceedings*, *17th ASCE Engineering Mechanics Conference*, University of Delaware, Newark, Delaware, 13–16 June 2004. CD-ROM.
[16] M. Gürgöze, Proportionally damped systems subject to damping modifications by several viscous dampers, *Journal of Sound and Vibration* 255 (2002) 407–412.
[17] B.M. Pacheco, Y. Fujino, A. Sulekh, Estimation curve for modal damping in stay cables with viscous damper, *Journal of Structural Engineering* 119 (1993) 1961–1979.
[18] P.D. Cha, W.C. Wong, A novel approach to determine the frequency equations of combined dynamical systems, *Journal of Sound and Vibration* 219 (1999) 689–706.